ELSEVIER

Journal of Power Sources 81–82 (1999) 373–377

JOURNAL OF POWER SOURCES

www.elsevier.com/locate/jpowsour

The study of irreversible capacity in lithium-ion anodes prepared with thermally oxidized graphite

Robert S. Rubino *, Esther Sans Takeuchi

Wilson Greatbatch Ltd., 10,000 Wehrle Drive, Clarence, NY 14031, USA

Abstract

The effect of thermal oxidation on the anodic characteristics of graphite was investigated. This treatment led to a large increase in irreversible capacity which was attributed to the expansion of pores in the graphite. Variations in the electrolyte were found to significantly affect the magnitude of this increase. A comparison of various electrolytes was used to study the irreversible reduction reactions which take place at the anode during the first cycle of a lithium-ion cell.

Keywords: Lithium-ion batteries; Irreversible capacity; Passivation layer

1. Introduction

Graphite is an attractive material for lithium-ion anodes because of its high theoretical capacity (372 mAh/g), low first cycle capacity loss, and good cycle life [1]. It is possible that these properties may be further enhanced by appropriate modification of the graphite. Oxidation of graphite, both chemically and thermally, has been reported to increase the anode capacity while simultaneously reducing the first cycle capacity loss [2–4]. It was our desire to improve graphite material by optimizing a thermal oxidation process.

2. Experimental

Synthetic graphite (LK-702, Nippon Carbon) was oxidized by heating at 550°C under air for various lengths of time (6–56 h). The change in weight (% burn-off) was determined for each graphite as a measure of the extent of oxidation.

BET surface area was measured with a Micromeritics Gemini III 2375 using nitrogen as the adsorbent. Methylene Blue surface area was measured by stirring graphite (40 mg) in a methylene blue solution (2×10^{-5} M, 0.2% Triton-X) for 20 h. After centrifugation, the change in concentration was determined spectrophotometrically with a Milton Roy Spectronic 1001 Plus ($\lambda = 661$ nm). Surface area calculations were based on a value of 170 $Å^2$ per molecule of methylene blue.

Elemental analyses for hydrogen and oxygen were done by Laboratory Testing (Dublin, PA).

X-ray diffraction studies were conducted at the State University of New York at Buffalo using Cu K_α radiation ($\lambda = 1.5406$ Å). Data were collected between 25° and 80° (2θ) at intervals of 0.02°. Crystallite dimensions were calculated using the Scherrer equation [5].

Anodes were prepared by combining graphite, PVDF (Aldrich, 9 wt.% in DMF), and sufficient DMF to make a slurry. The amount of PVDF solution added was such that the final electrode would be 8% binder by weight. The mixture was coated onto copper foil (0.001 cm thickness) using the doctor blade technique. The electrodes were then dried (105°C under vacuum) for 16 h and compressed (0.3 t/cm^2).

Graphite anodes (4×2.5 cm) were tested in half-cells versus lithium with a lithium reference electrode. Both lithium electrodes (3.5×5 cm) were prepared by brushing lithium foil onto nickel leads. The three electrodes were separated with 30 μm thick polyethylene separator and then were rolled onto a small cylinder (1.5 cm diameter). This cylinder was inserted into a larger cylinder (2.25 cm diameter) which was capped with a septum and vacuum-filled with electrolyte.

Electrolyte components were obtained commercially and were used without further purification. EC, DMC, $LiPF_6$,

* Corresponding author. Tel.: +1-716-759-5586; Fax: +1-716-759-5480; E-mail: rrubino@greatbatch.com

0378-7753/99/$ - see front matter
PII: S0378-7753(99)00217-7

and $LiBF_4$ were purchased from EM Industries, $LiAsF_6$ was purchased from FMC.

Capacities were determined by cycling between 1.5 and 0.02 V at a rate of 0.5 mA/cm^2 on a MACCOR Series 4000 test system. Reversible capacity was defined as the second intercalation capacity. Irreversible capacity was defined as the difference between the first and second intercalation capacities.

Depth-of-discharge studies were conducted by sequentially cycling an individual cell as follows: 1.5–0.8 V (5 times), 1.5–0.5 V (5 times), 1.5–0.2 V (5 times), 1.5–0.1 V (5 times), and 1.5–0.005 V (5 times). The difference between the first and fifth intercalation capacity represents the total irreversible capacity in a particular voltage range. Since the coulombic efficiency typically approaches 100% by the fifth cycle in each range, any additional irreversible capacity realized after reducing the cut-off voltage is solely the result of processes which occur between that voltage cut-off and the preceding one.

3. Results and discussion

By varying the length of the oxidation procedure, five new materials were obtained. The graphites were characterized as having 1.4, 5.2, 9.3, 16.2 and 20.7% burn-off. There was a nearly linear correlation between oxidation time and burn-off. The treated graphites were then evaluated as lithium-ion anodes with 1 M $LiPF_6$ (30:70 EC/DMC) electrolyte.

The reversible and irreversible capacities of the graphites are shown in Fig. 1. As expected, oxidation increased the reversible capacity, but the magnitude of the effect was small. Even at over 20% burn-off, the reversible capacity climbed less than 2% from 311 mAh/g for the untreated graphite to 318 mAh/g. This is much smaller than the 10–30% benefit reported by Peled et al. for the graphite types that they studied [2].

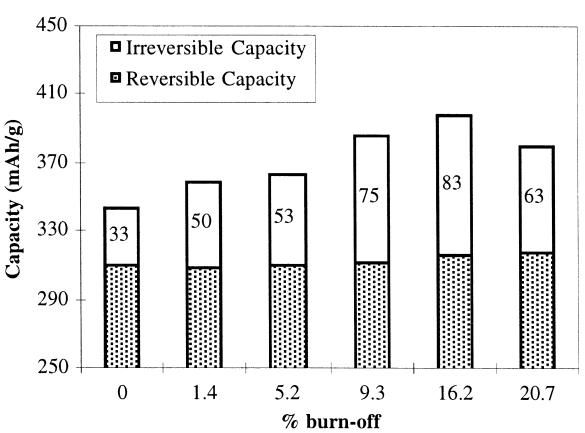

Fig. 1. First cycle intercalation capacities of the five oxidized graphites and a control. The value labels represent the irreversible capacities. Electrolyte = 1 M $LiPF_6$ (30:70 EC/DMC).

Table 1
Elemental analysis for hydrogen and oxygen (wt.%)

Graphite	Hydrogen	Oxygen
LK-702	0.005	0.051
16% burn-off	0.002	0.049

Irreversible capacity, however, was significantly influenced by the graphite pre-treatment. As the amount of burn-off increased, the irreversible capacity went from 33 mAh/g for the untreated graphite to a maximum of 83 mAh/g at 16.2% burn-off. At the highest level of burn-off (20.7%), the trend reversed, but the irreversible capacity remained substantially elevated. These results were surprising since we had expected oxidation to result in decreased irreversible capacity.

Irreversible capacity can be the result of several 'side' reactions within the cell. In some less ordered carbons, reduction of functionality on the carbon surface can make up a substantial portion of irreversible capacity [6,7]. This is not likely to be the case with graphite because it typically has limited surface area and therefore little functionality. Thermal oxidation may increase the concentration of surface oxides thereby increasing the irreversible capacity [8]. Elemental analysis for hydrogen and oxygen was done to test this hypothesis (Table 1).

A comparison of untreated graphite to oxidized material (16% burn-off) shows virtually no difference in oxygen content. Hydrogen content decreased, suggesting a migration towards functional groups which are at a higher oxidation state (e.g., lactones, carboxylates). In both cases, the oxygen content is so small that if one assumes that each oxygen atom is capable of oxidizing two moles of lithium, the contribution to irreversible capacity would be only 1.7 mAh/g. Therefore, reduction of surface oxides does not make a significant contribution to irreversible capacity in these materials.

The process most commonly associated with irreversible capacity is the reaction between lithium-intercalated carbon and the electrolyte. This reaction continues until a passivation layer composed of reaction byproducts is formed on the electrode. The passivation layer functions as an ionic conductor and an electronic insulator allowing free movement of ions, but preventing further decomposition of the electrolyte. The amount of lithium consumed during the formation of this layer depends on the amount of surface area, the reactivity of the surface, and the efficiency of the passivation layer.

Several authors have observed a correlation between irreversible capacity and surface area [9,10]. Fig. 2 shows both the BET nitrogen and methylene blue surface areas for each graphite in this study. Because methylene blue is much bigger than nitrogen it cannot access some of the small pores that nitrogen can. A comparison of the two surface area measurements can provide information about the porosity of the sample.

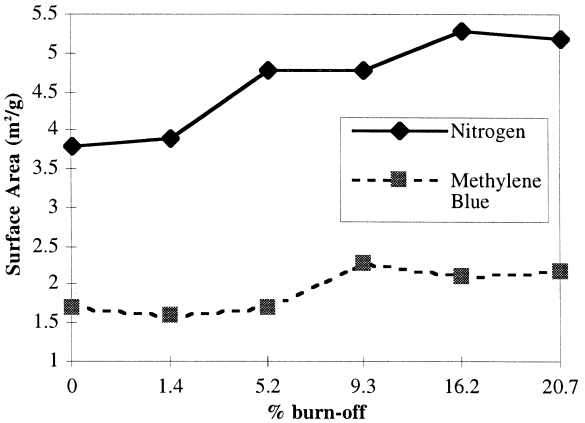

Fig. 2. BET nitrogen and methylene blue surface areas for oxidized graphites.

Both adsorbents indicated a trend toward more surface area as oxidation time was increased. This may be the result of reduced particle size or increased porosity. The fact that methylene blue did not show a significant response until 9.3% burn-off versus 5.2% for nitrogen indicates that pore access is at least partly responsible for the increased surface area.

Further evidence for the enhanced porosity of oxidized graphites comes from measurements of changes in the crystallite size. X-ray diffraction was used to determine the L_c and L_a dimensions for each of the graphites in this study. The L_a dimension was calculated from the [100] diffraction peak.

In Fig. 3, one can see that oxidation caused the crystallites to shrink along the axis parallel to the layer planes (L_a). There was little or no change in the perpendicular axis (L_c). This indicates that burn-off occurs primarily from the cross-sectional faces of the crystallites. The unused bonding orbitals of the carbons along these faces make them very susceptible to oxidation. At high temperatures such as those used in this study, the oxidized edge carbons will be vaporized to form carbon monoxide and carbon dioxide. New edge carbons will be exposed, oxidized, and vaporized, etc.

As a result of the shrinking of the crystallites, the small pores between adjacent crystallites will become larger. Electrolyte components will achieve access to these pores and, therefore, the surface requiring passivation will be expanded.

A similar result was reported by Xue and Dahn for hard carbons [11]. They proposed that oxidation caused a widening of the pore openings resulting in large increases in irreversible capacity. In the case of turbostratic carbons, surface area climbs rapidly as external pores are opened because of the inherently porous nature of the interior of the particles. With graphite, one sees only a 50% increase in surface area at 15–20% burn-off because the pores being opened lead to a highly ordered, nonporous interior.

The 250% increase in irreversible capacity at 16.2% burn-off cannot be solely the result of increased surface area. The reactivity of the new surfaces formed must also be taken into consideration. A study by Winter et al. showed that the ratio of basal to cross-sectional surface is related to irreversible capacity in graphites [9]. They propose that cross-sectional surface area requires a thicker passivation layer (SEI) than the relatively less reactive basal surface. Therefore, graphites with greater proportions of cross-sectional surface have higher irreversible capacity.

We propose that much of the new surface formed as a result of oxidation is cross-sectional in nature (Fig. 4). Prior to oxidation, the spaces between the crystallites are small and may contain disordered areas of carbon. Therefore, electrolyte is mainly exposed to basal faces with minimal passivation requirements. As the crystallites shrink, pores are formed which are lined with cross-sectional surface. Electrolyte entering these pores will be reduced until a thick passivation layer is formed. The energy requirements of forming a thicker passivation layer result in higher irreversible capacity.

Although oxidation fails to improve the anodic characteristics of the graphite, the oxidized graphites are a useful tool for studying the irreversible reactions which take place at the anode. By varying the extent of graphite oxidation in a given electrolytic system, it is possible to isolate the portion of the irreversible capacity which is the result of surface passivation.

For example, a depth-of-discharge study (see Section 2) was conducted in order to correlate the passivation reactions with a particular voltage. In this study, irreversible capacity was measured as a function of voltage for untreated graphite as well as two oxidized materials (Table 2). All of the materials performed similarly except during discharge to 0.2 V. The total irreversible capacity between 0.5 and 0.2 V climbed tenfold from 2.5 mAh/g for untreated LK-702 to 24.3 mAh/g at 16.2% burn-off.

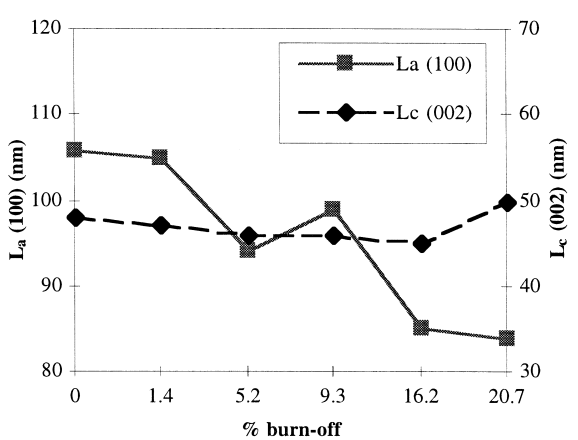

Fig. 3. Crystallite dimensions for oxidized graphites in nm. The numbers in parentheses represent the diffraction peak from which the lattice dimension was calculated.

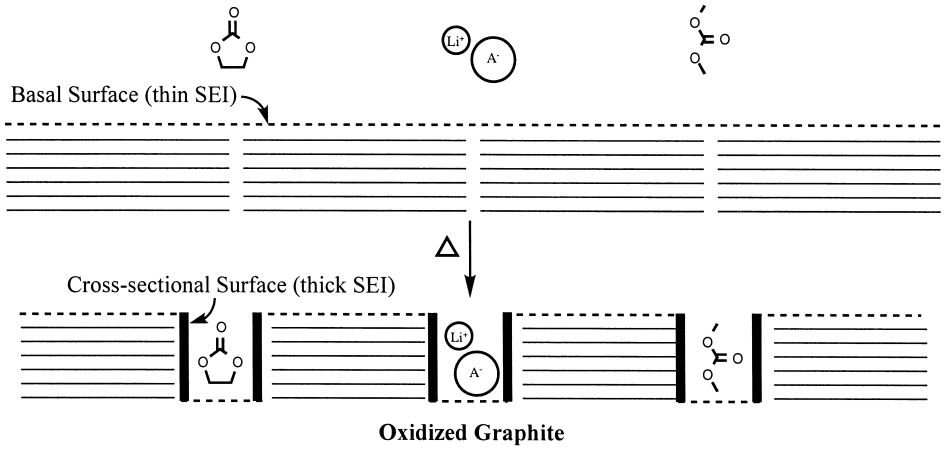

Fig. 4. A conceptual model of oxidized graphite. In the top picture, solvent and electrolyte salt cannot enter spaces between crystallites and are exposed only to basal faces. In the oxidized graphite, narrower crystallites allow electrolyte between them, resulting in exposure to highly reactive cross-sectional faces.

Therefore, the increased surface passivation reactions between the electrode and electrolyte take place primarily between 0.5 and 0.2 V in this system.

Besides the anode material, electrode passivation is highly dependent on the electrolyte composition. Good electrolytes react minimally with the anode to form a highly stable and effective passivation film. Much work has been done to determine the composition of the passivation layer in a variety of electrolyte systems [12–15]. By changing the electrolyte in cells containing a range of oxidized graphites, it is possible to measure the changes in the passivation characteristics of the electrode. This allows one to make conclusions about which electrolyte components are most responsible for passivating the electrode.

Table 3 shows the results of replacing $LiPF_6$ with $LiAsF_6$ and $LiBF_4$. Cells containing $LiBF_4$ were similar to those containing $LiPF_6$ in that irreversible capacity increased as the graphite became more porous. The increase was particularly intense between 0.5 and 0.1 V.

When cells were prepared with $LiAsF_6$, however, there was virtually no change in irreversible capacity for any of the graphites. This suggests that salt reduction is a major passivation reaction in $LiPF_6$ and $LiBF_4$ electrolytes since replacement of these salts has a dramatic effect. It may be that these salts enter the pores formed by oxidation, as shown in Fig. 4, and are reduced at the cross-sectional surface until an effective passivation layer is formed.

The reason why $LiAsF_6$-electrolyte does not respond in a similar manner is unclear. The nearly linear correlation between irreversible capacity and graphite surface area with this electrolyte suggests that $LiAsF_6$ is not responding to the change in the reactivity of the newly formed surface. Perhaps reduction of this salt forms a very efficient passivation layer on cross-sectional surfaces such that it is similar in thickness to that formed on basal surfaces. Alternatively, the relatively large size of AsF_6^- may prevent it from entering the pores. In any case, the amount of irreversible capacity above 0.8 V in $LiAsF_6$-containing cells indicates that this salt is reduced at a higher voltage than the other two.

The contributions of solvent reduction to irreversible capacity must also be considered. Like salt, solvent is also exposed to expanded, more reactive surfaces in oxidized graphites. The passivation reactions involving solvent should also be magnified in these materials. However,

Table 2
Irreversible capacity (mAh/g) as a function of voltage for three graphite materials (1.0 M $LiPF_6$, 30:70 EC/DMC). Negative values indicate that the 5th cycle intercalation capacity was more than the 1st cycle intercalation capacity

Voltage	LK-702	5.2%	16.2%
1.5–0.8	2.5	2.2	2.1
0.8–0.5	5.4	5.4	6.5
0.5–0.2	2.5	8.8	24.3
0.2–0.1	−2.9	−4.6	0.1
0.1–0.005	6.5	6.3	9.0

Table 3
Irreversible capacity (mAh/g) as a function of voltage for cells with $LiAsF_6$ and $LiBF_4$ electrolyte (1 M, 30:70 EC/DMC)

Voltage	LK-702	5.2%	16.2%
$LiAsF_6$			
1.5–0.8	10.2	12.8	14.6
0.8–0.5	3.4	3.8	4.0
0.5–0.2	4.5	6.4	6.5
0.2–0.1	−5.3	−10.7	−8.7
0.1–0.005	6.3	6.6	11.2
$LiBF_4$			
1.5–0.8	2.6	2.2	2.1
0.8–0.5	11.3	15.9	24.2
0.5–0.2	14.6	39.0	71.3
0.2–0.1	2.6	10.5	16.5
0.1–0.005	17.4	21.2	34.6

Table 4
Irreversible capacity (mAh/g) as a function of voltage for cells with 50:50 EC/DMC and 10:90 EC/DMC electrolyte (1 M, $LiAsF_6$)

Voltage	LK-702	5.2%	16.2%
50:50 EC/DMC			
1.5–0.8	11.6	11.8	15.1
0.8–0.5	4.0	4.1	5.8
0.5–0.2	8.0	29.7	49.8
0.2–0.1	−15.0	−2.8	6.8
0.1–0.005	7.6	10.8	25.1
10:90 EC/DMC			
1.5–0.8	13.9	12.6	15.3
0.8–0.5	3.7	3.2	3.3
0.5–0.2	4.5	5.8	5.2
0.2–0.1	−6.0	−0.8	5.7
0.1–0.005	1.2	7.1	10.7

when salt reductions are minimized as in the case of $LiAsF_6$-electrolyte (30:70 EC/DMC), it allows one to see that solvent reduction reactions do not appear to increase in anodes containing oxidized graphites.

It appears that 30:70 EC/DMC reacts slowly with the electrode such that the electrode is preferentially passivated by the more rapid salt reduction. This may be true for all graphite surfaces, or just for the newly formed cross-sectional surfaces. XPS studies on HOPG by Bar-Tow et al. have shown that salt reduction products predominate on the cross-sectional surface [14].

Table 4 shows what happens when the electrolyte solvent ratio is changed. For this study, $LiAsF_6$ was used in order to reduce the effects of the salt. When the EC concentration was reduced to 10%, there was no change in cell performance. The irreversible capacity increased only modestly when oxidized graphite was used.

At an EC concentration of 50%, however, irreversible capacity became highly dependent on the extent of graphite oxidation. At 16.2% burn-off, a multifold increase was observed at all three voltage ranges between 0.5 and 0.005 V. By raising the EC percentage, solvent reduction became competitive with salt reduction. Entry of solvent into the pores and the subsequent reduction at the cross-sectional surfaces can be easily observed in this system.

4. Conclusions

Thermal oxidation of graphite resulted in large increases in irreversible capacity. It is believed that surface pores between adjacent crystallites became larger as a result of the treatment, increasing the surface area of the graphite. The need to passivate this additional surface, which was primarily of the highly reactive cross-sectional type, led to the increased irreversible capacity.

Changing the electrolyte salt to $LiAsF_6$ substantially reduced the reaction between the electrolyte and the oxidized graphites. We conclude, therefore, that reduction of electrolyte salt is a major passivation reaction at cross-sectional surfaces in systems containing $LiPF_6$ and $LiBF_4$ (30:70 EC/DMC). Depth-of-discharge studies were able to correlate the reduction of these salts with particular voltage ranges (0.5–0.2 V for $LiPF_6$; 0.5–0.1 V for $LiBF_4$).

When the electrolyte solvent contained 30% or less of EC, reduction of solvent was a minor passivation process at the surfaces formed by oxidation. By increasing the EC concentration to 50%, solvent reactions with the electrode became competitive with salt reactions. These solvent reactions, which probably consist primarily of the reduction of EC, were most prevalent between 0.5 and 0.005 V.

References

[1] J.R. Dahn, A.K. Sleigh, H. Shi, B.M. Way, W.J. Weydanz, J.N. Reimers, Q. Zhong, U. von Sacken, Lithium Batteries. New Materials, Developments and Perspectives, Elsevier, 1994, 1–47.
[2] E. Peled, C. Menachem, D. Bar-Tow, A. Melman, J. Electrochem. Soc. 143 (1996) L4.
[3] C. Menachem, E. Peled, L. Burstein, Y. Rosenberg, J. Power Sources 68 (1997) 277.
[4] Y. Ein-Eli, V.R. Koch, J. Electrochem. Soc. 144 (1997) 2968.
[5] K. Kinoshita, Carbon, Electrochemical and Physicochemical Properties, Wiley, 1988, 32.
[6] W. Xing, J.R. Dahn, J. Electrochem. Soc. 144 (1997) 1195.
[7] M. Kikuchi, Y. Ikezawa, T. Takamura, J. Electroanal. Chem. 396 (1995) 451.
[8] D. Rivin, Rubber. Chem. Technol. 44 (1971) 307.
[9] M. Winter, P. Novak, A. Monnier, J. Electrochem. Soc. 145 (1998) 428.
[10] R. Fong, U. von Sacken, J.R. Dahn, J. Electrochem. Soc. 137 (1990) 2009.
[11] J.S. Xue, J.R. Dahn, J. Electrochem. Soc. 142 (1995) 3668.
[12] R. Imhof, P. Novak, J. Electrochem. Soc. 145 (1998) 1081.
[13] D. Aurbach, B. Markovsky, A. Shechter, Y. Ein-Eli, H. Cohen, J. Electrochem. Soc. 143 (1996) 3809.
[14] D. Bar-Tow, E. Peled, L. Burstein, Proc. Electrochem. Soc. 18 (1997) 324.
[15] E.S. Takeuchi, H. Gan, M. Palazzo, R. Leising, S. Davis, J. Electrochem. Soc. 144 (1997) 1944.